Very Low-Frequency Electromagnetic Method: A Shallow Subsurface Investigation Technique for Geophysical Applications

S. P. Sharma, Arkoprovo Biswas and V. C. Baranwal

Abstract The very low-frequency (VLF) electromagnetic (EM) method is the simplest EM method to delineate shallow subsurface conducting structures. Since the approach utilizes signals transmitted from worldwide transmitters located in coastal areas in the 5–30 kHz frequency band, it is suitable to depict conducting structures up to 200 m depth in highly resistive terrain. Freely and readily available primary field signals anywhere around the Earth make the VLF method very convenient and efficient for field data collection. Further, VLF data processing using digital linear filtering is quite accurate and very efficient in depicting the qualitative information about subsurface conductors, even though quantitative interpretation of VLF data is as complex as other EM data interpretation. In the present study, various aspects of the VLF method such as basic theory, worldwide VLF transmitters, quantities measured, and interpretation procedures are discussed in detail. Finally, the efficacy of the VLF method for groundwater investigation, mineral investigation, and landslide and subsurface pollution monitoring studies has been demonstrated. Even though the VLF method is a rapid technique for subsurface investigation, use of complementary geophysical methods such as gravity, direct current (DC) resistivity, self-potential, radiometric, etc., reduces the ambiguity in the interpretation and yields reliable subsurface information.

Keywords VLF electromagnetic · Groundwater and mineral investigation · Landslide studies · Subsurface pollution studies

1 Introduction

Electromagnetic (EM) method of geophysical prospecting deals with the propagation of low-frequency time varying EM field (primary field) into the earth. Such fields are generated by passing alternating current in a number of transmitters (a

S. P. Sharma (✉) · A. Biswas
Department of Geology and Geophysics, IIT Kharagpur, Kharagpur, West Bengal 721302, India
e-mail: spsharma@gg.iitkgp.ernet.in

V. C. Baranwal
Geological Survey of Norway (NGU), Trondheim, Norway
e-mail: vikas.baranwal@ngu.no

D. Sengupta (ed.), *Recent Trends in Modelling of Environmental Contaminants,*
DOI 10.1007/978-81-322-1783-1_5,

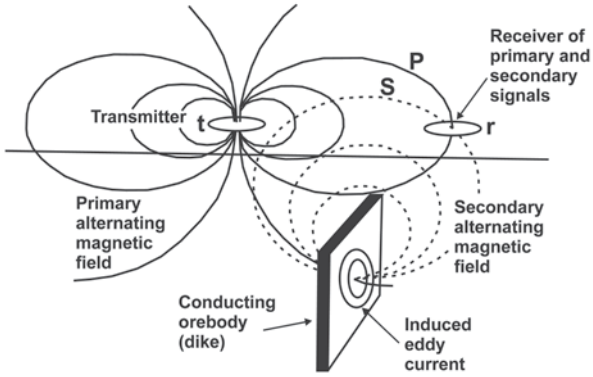

Fig. 1 General principle of electromagnetic (EM) surveying

small circular loop, a large rectangular loop, a grounded wire, a long vertical cable, etc.). Due to low frequency, the EM field penetrates into Earth's interior and interacts with subsurface conductors. Due to this interaction, according to Faraday's law of EM induction, an induced electromotive force (emf) is generated in the subsurface conductor. Further, an induced current is set up in the subsurface conductor. This induced current (secondary current) produces a secondary field (Fig. 1) which propagates to the earth's surface. On the Earth's surface a vector combination of the primary and secondary fields is recorded. The whole process is governed by the well known Maxwell's equations (Faraday's and Ampere's laws) and is known as EM induction phenomenon in the earth.

EM methods utilize a broad frequency range (1 GHz to 10^{-6} Hz). Ground penetrating radar (GPR) uses the highest frequency in the band of 25 MHz to 1 GHz. However, GPR method is based on reflection principle, and EM induction does not take place at such a high frequency. Very low-frequency (VLF) EM method uses the frequency band 5–30 kHz. Audio frequency magnetic field method which is based on thunderstorm (lightening) activity has a frequency of 1–1,000 Hz. Controlled source EM method that uses transmitter and receiver in field used a frequency range of 100–5,000 Hz. Magnetotelluric method which is based on ionosphere current has the lowest frequency of $1–10^{-6}$ Hz or even smaller. Depth of investigation is frequency dependent and increases in the order mentioned above.

Transmitter is a very important component in EM surveying. VLF method has advantage in this regard, as transmitters are freely available for measurement. In principle, the VLF method uses transmitter located in coastal areas worldwide. The primary aim of these transmitters is long distance marine communication or communication with submarines. These signals travel worldwide between the Earth's surface and ionosphere; hence, these signals travel thousands of kilometer distances without much attenuation, as their frequencies are in the lower band (5–30 kHz) in comparison to the normal communication frequencies (thousands of kHz to GHz range). Therefore, they are referred to as VLF methods, even though they use the highest frequency in EM methods based on EM induction phenomenon.

Figure 2 shows a schematic diagram of the working principle of VLF EM method. Primary field from the transmitter travels intercontinental distances, and mea-

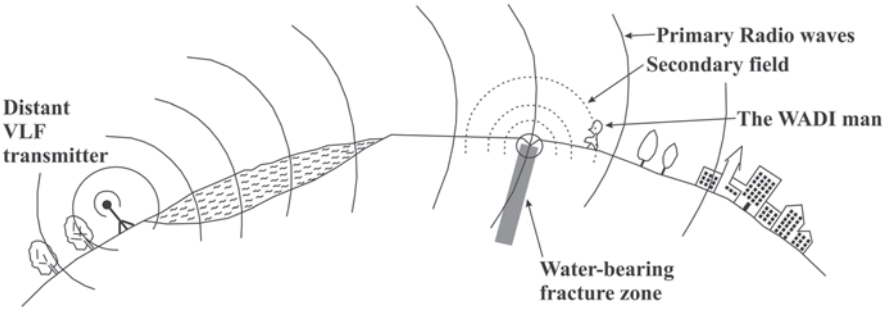

Fig. 2 Basic principle of VLF method. (Source ABEM, Wadi)

surements are performed in uniform primary time varying magnetic field in a small survey area.

2 VLF Transmitters

VLF transmitters are basically long grounded vertical wires of several hundred meters length, carrying alternating current, and operating as vertical electrical dipole with a transmitting power of the order of 1 MW. The monopole transmitting antennas are electrically very small in comparison to the wavelength at VLF frequencies which is of the order of 15 km. An addition of "top-loading," which consists of enormous horizontal wire arrays located at (and connected to) the top of the antenna is required to get high transmission power in the order of 1 MW (McNeill and Labson 1991). Therefore, VLF transmitters, in general, are large, complicated, and expensive structures. These transmitters are set for communication with submarines, and the VLF method takes advantage of the transmitted EM fields by using them as primary field source. Table 1 shows a list of the transmitters working in the VLF range worldwide.

The EM fields transmitted from VLF transmitters at a large distance are a combination of ground and sky waves. Ground wave travels over the earth's surface, whereas the sky wave is refracted and reflected by the ionized layers in the upper atmosphere (~50 km and higher). Since the power of a transmitter is very large (~1 MW), it is possible to detect these fields over continental distances, nearly half way around the world. The magnetic field lines are horizontal circles concentric about the transmitter. At distances of several hundred kilometers, this field is practically uniform and at right angles to the transmitter direction which leads to assumption of the plane wave (Fig. 3). There is no guarantee to receive enough strong VLF fields everywhere in the world due to inaccessibility of proper transmitter for some regions and also sometimes the VLF stations may be switched off due to maintenance work. Therefore, using portable VLF transmitters may be an alternative for such regions.

Table 1 VLF stations with operating frequency and their locations

Frequency (kHz)	Stations	Frequency (kHz)	Stations	Station code	Place	Country	Latitude	Longitude
15.1	FUO HWUVTI	22.8	NWC	3SA	Changde	China	29N04	111E43
15.3	NHB NPN NPM NLK NEJ	22.9	JJI	3SB	Datong	China	39N56	113E15
15.5	NWC NPM NAA NSS	23.3	JJI	DHO	Burlage	Germany	53N05	007E37
15.6	EWB	23.4	NPM	EWB	Odessa	Ukraine	46N29	030E44
15.7	NPM NSS NAK NPL NPG	24.0	NPM BA NSS NLK	FTA	Assise	France	48N32	002E34
16.0	GBR	24.8	NLK	FUO	Croix	France	44N45	000W48
16.2	UGK JAP	25.3	NAA	GBR	Rugby	UK	52N22	001W11
16.3	VTX	25.5	3SB	GBZ	Rugby	UK	52N22	001W11
16.4	JXN	25.8	NSS NAA	GQD	Rugby	UK	52N22	001W11
16.6	NPM NSS NAK	26.1	NPM NLK NPG NEJ	HWU	Le Blanc	France	46N37	001E05
16.8	FTA	27.0	RCV NAU	ICV	Tavolara	Italy	40N55	009E45
17.0	VTX	27.5	NAU	JAP	Yosami	Japan	34N58	137E01
17.1	UMS	27.7	3SB	JJH	Kure	Japan	34N14	132E34
17.4	NDT	28.0	DHO 3SB	JJI	Ebino	Japan	32N05	131E51
17.6	JXZ	28.5	NAU NPL	JXN	Helgeland	Norway	66N25	013E01
17.8	NPM NAA NSS	28.6	RAM	JXZ	Helgeland	Norway	66N25	013E01
17.9	UBE	29.0	3SA	NAA	Cutler ME	USA	44N39	067W17
18.0	NBA NPL NPG NLK	30.0	UNW	NAK	Annapolis	USA	38N59	076W28
18.1	UPD	21.0	3SA	NAU	Aguada	Puerto Rico	18N23	67W11
18.2	VTX NSS JJH	21.2	JJI	NBA	Balboa	Panama	09N04	079W39
18.3	HWU	21.4	NPM NAA NSS	NDT	Yokosukaichi	Japan	34N58	137E01
18.5	DHO NAA	21.6	3SB	NEJ	Seattle	USA	47N41	122W15
18.5	NHB NPN NPM NAA NLK NPG NEJ	21.8	TBA	NHB	Kodiak	Alaska	57N45	152W30
18.7	JJI	21.9	JJI	NLK	Oso Wash	USA	48N12	121W00
18.9	UMB	22.2	JJI	NPC	Seattle	USA	47N35	122W32
19.0	GQD NPM NSS	22.3	NWC NAA NLK NPC NSS NPM	NPG	S Francisco	USA	38N06	122W16

Table 1 (continued)

Frequency (kHz)	Stations	Frequency (kHz)	Stations	Station code	Place	Country	Latitude	Longitude
19.1	JJI	22.6	GBR	NPL	S Diego	USA	32N44	117W05
19.2	VTX	22.8	NWC	NPM	Pearl Harbor	Hawai	21N25	158W09
19.4	NHB NPN NPM NEJ NLK	22.9	JJI	NPN	Guam	Guatemala	13N34	144E50
19.5	3SA	23.3	JJI	NSS	Washington	USA	38N59	076W27
19.6	GBZ	23.4	NPM	NWC	North West Cape	Australia	21S47	114E09
19.8	NWC NPM NLK NPL NPG TBA	24.0	NPM NBA NSS NLK	RAM	Moscow	Russia	55N49	037E18
19.9	JJI	24.8	NLK	RCV	Rostov	Russia	47N18	039E48
20.2	JJI ICV	25.3	NAA	TBA	Antalya	Turkey	36N53	030E43
20.3	JJI	25.5	3SB	UBE	Petrolovsk	Russia	52N59	158E39
20.5	SA 3SB	25.8	NSS NAA	UGK	Kaliningrad	Russia	54N42	020E30
20.8	ICV	26.1	NPM NLK NPG NEJ	UMB	Rostov	Russia	57N14	039E48
21.0	3SA	27.0	RCV NAU	UMS	Moscow	Russia	55N49	037E18
21.2	JJI	27.5	NAU	UNW	Kaliningrad	Russia	54N45	020E30
21.4	NPM NAA NSS	27.7	3SB	UPD	Murmansk	Russia	68N58	033E05
21.6	3SB	28.0	DHO 3SB	VTI	Bombay	India	19N00	073E00
21.8	TBA	28.5	NAU NPL	VTX	Vijayanagaram	India	08N26	077E44
21.9	JJI	28.6	RAM					
22.2	JJI	29.0	3SA					
22.3	NWC NAA NLK NPC NSS NPM	30.0	UNW					
22.6	GBR							

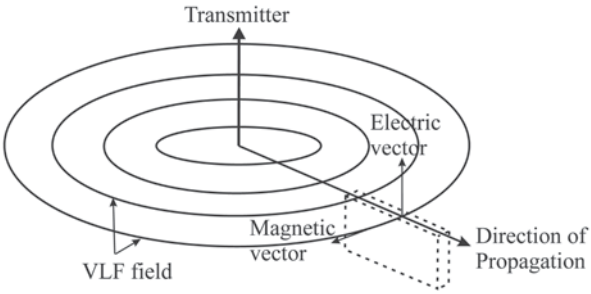

Fig. 3 Principle of VLF EM method. *Dashed lines* show a conductor striking towards the transmitter which is cut by the magnetic vector of the EM field

3 VLF and VLF-R Anomalies

3.1 E-Polarization

If y-axis is the strike direction and VLF transmitter is located in y-direction, then tilt angle α, which is the inclination of the major axis of the polarization ellipse, and the ellipticity e, which is the ratio of the minor to the major axis of the ellipse, are calculated by the formulae (Smith and Ward 1974)

$$\tan 2\alpha = \pm \frac{2(H_z/H_x)\cos\Delta\phi}{1-(H_z/H_x)^2} \tag{1}$$

and

$$e = \frac{H_z H_x \sin\Delta\phi}{H_1^2}. \tag{2}$$

where H_z and H_x are the amplitudes, and the phase difference $\Delta\phi = \phi_z - \phi_x$, in which ϕ_z is the phase of H_z, and ϕ_x is the phase of H_x, and $H_1 = |H_z e^{i\Delta\phi} \sin\alpha + H_x \cos\alpha|$. The tangent of the tilt angle and the ellipticity are good approximations to the ratio of the real component of the vertical secondary magnetic field to the horizontal primary magnetic field, and to the ratio of the quadrature component of the vertical secondary magnetic field to the horizontal primary field, respectively (Paterson and Ronka 1971). These quantities are called the real (=tan $\alpha \times 100\%$) and imaginary ($= e \times 100\%$) anomalies, respectively, and are normally expressed in percentage.

A VLF-R measurement records the horizontal electric field component and an orthogonal horizontal magnetic field. It is possible to use both the E- and H-polarization. In E-polarization mode, the electric field is measured in a direction parallel to the geological strike. The apparent resistivity ρ_a and phase angle φ computed from horizontal electric field E_y and magnetic field H_x are given by the formulae (e.g., Kaikkonen 1979):

$$\rho_a = \frac{1}{\omega\mu}\left|\frac{E_y}{H_x}\right|^2 \tag{3}$$

and

$$\phi = \arctan\left[\frac{\mathrm{Im}\left(\frac{E_y}{H_x}\right)}{\mathrm{Re}\left(\frac{E_y}{H_x}\right)}\right] \tag{4}$$

3.2 H-Polarization

In H-Polarization mode, real and imaginary VLF anomalies do not exist and they are considered as zero.

For H-polarization measurement, the VLF transmitter should be located in a direction perpendicular to the geological strike, the electric field is measured in a direction perpendicular to the geological strike, and the magnetic field in the direction of the strike. Expressions for apparent resistivity and phase is given by

$$\rho_a = \frac{1}{\omega\mu}\left|\frac{E_x}{H_y}\right|^2 \tag{5}$$

$$\phi = \arctan\left[\frac{\mathrm{Im}\left(\frac{Ex}{Hy}\right)}{\mathrm{Re}\left(\frac{Ex}{Hy}\right)}\right] \tag{6}$$

For theoretical computations, the field components Ex and E_y are obtained by applying the finite element technique with the Galerkin process directly to the Maxwell's equations, and other field components can be computed from Maxwell's equations by numerical differentiation. To solve the forward problem the magnetotelluric finite element program of Wannamaker et al. (1987) has been used after a slight modification for VLF purposes. For the details of the finite element modeling and VLF computation, papers by Kaikkonen (1979) and Wannamaker et al. (1987) are referred. Cubic spline interpolation (Press et al. 1992) is used to obtain response at the desired observation locations.

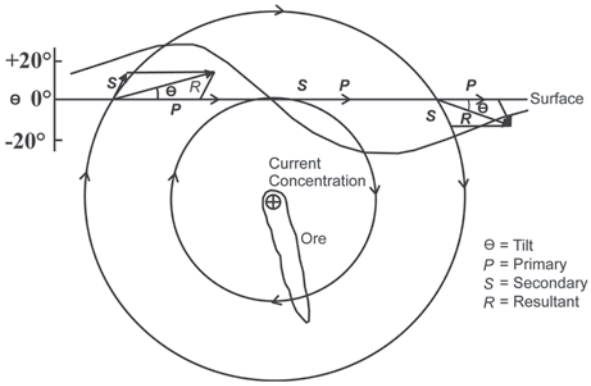

Fig. 4 Tilt-angle profiles resulting due to presence of a vertical conductor. (After Parasnis 1986)

Depth of Penetration or Skin Depth

In general, depth of penetration for EM fields is assumed to be equal to a skin depth value δ. The skin depth is the depth at which EM fields are attenuated to 1/e of its surface amplitude during the propagation through an isotropic earth. The value of skin depth depends on frequency f (in Hz) and effective resistivity ρ (in Ωm) which is a sort of average resistivity of an equivalent homogeneous subsurface to the actual subsurface. The expression for skin depth in meter is:

$$\delta = 503\sqrt{\frac{\rho}{f}}. \tag{7}$$

It is evident from Eq. (7) that the depth of penetration will be greater in a more resistive subsurface at the same frequency of EM fields and lower frequencies will achieve greater depth of penetration in same resistive subsurface. In a typical resistive medium (1,000 Ωm) the depth of investigation is less than 150 m at VLF frequencies.

4 Interpretation Procedures

In the presence of a single vertical conductive body, VLF real and imaginary anomalies change from negative to positive (or positive to negative depending on the convention of the sign used in the instrument) with a zero crossover exactly above the location of the vertical conductor (Fig. 4). Paterson and Ronka (1971) have discussed general nature of the tilt angle and ellipticity data in various situations. They demonstrated by numerical calculations that tilt angle and ellipticity data will be of opposite sign with approximately the same numerical value if a good conductor lies in a weakly conductive ground. However, tilt angle and ellipticity data will be of same sign with lower numerical value of ellipticity in comparison to tilt angle if a poor conductor lies in a non-conductive ground or on the surface.

It is easy to make qualitative interpretation of the location of conductive body in such simple cases, when a single conductor is present. The problem arises when more than one conductor are present along the same profile line. When many conductors are present in the subsurface then responses corresponding to these conductors couple together and it is difficult to decide about the location of each conductor separately.

Some researchers (Chouteau et al. 1996; Gharibi and Pedersen 1999; Becken and Pedersen 2003) have presented the mathematical techniques to transform the VLF data (real and imaginary anomalies) into VLF-R data (apparent resistivity and phase) for the interpretation. However, most common techniques to interpret the VLF data qualitatively are filtering techniques presented by Fraser (1969) and Karous and Hjelt (1983). Moreover, these filtering techniques do not provide exact depth information of the conductor. A more advanced filtering technique has been discussed by Pedersen and Becken (2005) to construct corresponding equivalent current density distribution images which also provides information about the depth of the conductor quantitatively. However, a fully quantitative interpretation in terms of resistivity and depth together can be obtained by various linearized and nonlinearized inversion schemes of VLF and VLF-R data.

4.1 Fraser Filtering Technique

Fraser (1969) presented a very simple filtering technique which performs phase shift of the tilt angle data by 90°, such that crossovers are transformed into peaks. The filtering process is simply performed by summing the observations at two consecutive data stations and then subtracting from the sum at the next two consecutive data stations. Mathematical formulation for the Fraser filtering is written as:

$$F(0) = (H_{-2} + H_{-1}) - (H_1 + H_2), \tag{8}$$

where H_{-2}, H_{-1}, etc., are the measured data (real or imaginary part of the magnetic transfer function) at consecutive stations with station interval Δx. $F(0)$ is filtered data obtained, corresponding to center of H_{-2} and H_2. If the VLF data is collected along parallel profile lines of same length and for the same transmitter, then filtered data can be contoured to locate the extension of the conductor in the survey area.

4.2 Karous–Hjelt Filtering Technique

Karous and Hjelt (1983) developed a filtering technique to calculate the equivalent current density which produces a magnetic field identical to the measured field. They applied the concept of linear filter theory to calculate apparent current density. According to the Biot–Savart's law, a magnetic field is produced by a current source. In case of VLF, we measure the secondary magnetic field which is pro-

duced by the eddy current set in the conductor by induction phenomenon. Therefore, Karous and Hjelt (1983) used this analogy and developed an efficient filter to calculate equivalent current density from the observed magnetic field. A number of filters of various lengths have been examined by Karous and Hjelt (1977), and a six point filter coefficient was found to be the shortest and most suitable within 8 % accuracy for the interpretation of the field of a single current source.

The application of this filtering technique is rather simple. The filter coefficients are multiplied with equi-spaced and consecutive observation points and then added to give the equivalent current density value at the centre of those observation points. This procedure is repeated by shifting filter coefficients to the next observation points until the last observation point along the profile. Therefore, first equivalent current density value is obtained for a location at the centre of second and third observation points, and the last equivalent current density value is obtained for a location at the centre of second and third observation points from the last station on the profile. The expression for the filtering technique is given as:

$$\frac{\Delta z}{2\pi} I_a(0) = -0.102H_{-3} + 0.059H_{-2} - 0.561H_{-1} + 0.561H_1 - 0.059H_2 + 0.102H_3 \tag{9}$$

where $I_a(0) = 0.5\left[I(\Delta x/2) + I(-\Delta x/2)\right]$ is the equivalent current density value. This filter is designed to be applied on equi-spaced data with the assumption that transformed current density values corresponds to the depth Δz, equal to the data spacing at which the current densities are to be calculated. Thus, it is possible to calculate the current distribution at different depths and to construct the equivalent current density cross-section from VLF data. However, it is important to note that the equivalent current density cross-section is a pseudo section which does not correspond to the actual current distribution. The relationship between the pseudo depth and the data interval Δx is a convention only, not a mathematical relationship.

Due to symmetry of the filter coefficients, it produces almost same features when applied on the real and imaginary components of the magnetic transfer function (Ogilvy and Lee 1991), therefore, generally current density cross-section generated by real component is used in the interpretation. A higher value of the current density shows presence of the conductor exactly below that location in the cross-section. The Karous–Hjelt filter is used for interpretation of VLF data collected from different regions.

4.3 Inversion of VLF and VLF-R Data

A quantitative interpretation of VLF or VLF-R data for depth and resistivity distribution can be carried out by applying various inversion schemes. In principle, approaches developed for the inversion of magnetotelluric (MT) data can be used to invert VLF and VLF-R data with slight modification in the forward modeling for computation of VLF responses.

Beamish (1994) used regularized inversion approach well known as OCCAM inversion to invert VLF-R data. The OCCAM inversion is developed by deGroot-Hedlin and ConsTable (1990) for inversion of 2-D MT data. Further, Beamish (2000) used 2-D MT inversion code developed by Rodi and Mackie (2001). Sharma and Kaikkonen (1998a, 1998b) have used very fast simulated annealing for inversion of VLF-R data. Kaikkonen and Sharma (1998) have also jointly inverted VLF and VLF-R data using very fast simulated annealing. A comparison of local and global inversion approaches for VLF and VLF-R data is discussed by Kaikkonen and Sharma (2001).

There are few literatures available on the inversion of VLF data. A 2-D OCCAM approach (deGroot-Hedlin and Constable 1990) works very well in a stable manner for inversion of VLF-R data. A further efficient variant of OCCAM inversion called REBOCC inversion developed by Siripunvaraporn and Egbert (2000) for MT data is used for inversion of VLF data (Oskooi and Pedersen 2005) and for the inversion of airborne VLF data (Oskooi and Pedersen 2006; Pedersen and Oskooi 2004). Monteiro Santos et al. (2006) have used a 2-D regularized inversion based on the approach of Sasaki (1989) to interpret single frequency VLF data.

5 Applications

5.1 Groundwater Exploration

Groundwater exploration in hard rock area is often challenging. Worldwide, hard rock areas are more problematic for the occurrence of groundwater than the soft rock areas. Groundwater movement in hard rock area takes place through fine fractures, and it is rather difficult to detect these fractures using a conventional direct current (DC) resistivity technique. Groundwater movement in hard rock areas forms vertical as well as dipping conductors and it could be delineated by VLF EM surveys. Therefore, VLF survey can be used to find the appropriate location and subsequently, resistivity survey can assist in verifying the suitability of the location.

An example for groundwater investigation from Purulia (WB), India is presented. The area belongs to Chhotanagpur Granite Gneiss Complex (CGGC). The area is characterized by gently dipping metamorphic rocks striking approximately in east–west direction. A ridge type structure with its axis approximately perpendicular to the strike of the formations, characterizes the area. The rock types in the area are granite gneiss, amphibolite, mica schist, quartzite, quartz vein, and calc-silicate rocks with interbanded crystalline limestone. A thin soil cover forms the upper surface of the study area which is followed by crystalline massive metamorphic rocks of very high resistivity. Exposure of hard rock can be seen at several isolated locations in the entire area. The surface exposure shows the strike of the formation approximately in the east–west direction and it is gently dipping. The most common rocks in the Purulia district are granites and granite gneiss in which metabasics occur as intrusives.

Integrated electrical and EM surveys were carried out in the hard rock areas of Purulia district (West Bengal), India, for delineation of groundwater-bearing zones that would be suitable for construction of deep tube-wells for large amounts of water. A detailed survey of the area was done using a VLF-WADI instrument and appropriate locations were selected for further study using Schlumberger resistivity sounding. Hence, the entire area was surveyed in a relatively short time by the combined use of resistivity and EM surveys.

Figure 5 shows the area map with detailed VLF profiles. From the various VLF profiles suitable locations were marked and subsequently resistivity surveys were performed. The VLF profile 0300E reveals the maximum amplitude in VLF anomaly. The real anomaly and apparent current density along this profile is shown in Fig. 6. It is important to mention that the entire area is almost flat and dry with hard rock exposure. However, the fracture has been depicted which is also confirmed with other electrical resistivity measurements such as profiling, self-potential measurement, as well as resistivity sounding (Sharma and Baranwal 2005). This location on VLF profile, 0300E, was drilled and a deep tube well is working successfully.

5.2 Mineral Exploration

Chromite Investigation

Chromite is a high density metallic mineral and it is often associated with mafic/ultramafic rock. Due to its high density, gravity method of prospecting is the best approach for its investigation. However, due to non-uniqueness in the interpretation, gravity method alone cannot be fully reliable. Since chromite is a metallic mineral, it possesses good electrical conductivity. Electrical and EM methods that deals with electrical conductivity of the subsurface are used in integrated study for the chromite investigation. Such an integrated study is performed around Tengarapada (Orissa), India (Fig. 7).

Major rock type present in the area sheared granite, quartzofeldspathic gneiss (QFG), and mafic/ultramafic rocks. Mafic/ultramafic rocks occur as pods that are aligned approximately parallel to a mylonitic shear zone that cuts through the QFG unit. Chromite is associated with these mafic/ultramafic rocks. The densities of chromites as well as mafic/ultramafic rocks are high. Therefore, mafic/ultramafic rock also can be interpreted as chromite from the gravity anomaly. However, chromite is electrically conducting but mafic/ultramafic rocks are highly resistive. Therefore, a VLF EM method is used to distinguish between these two high density materials.

The upper part of Fig. 8 shows measured VLF real and imaginary anomaly, and the lower part shows the current density section. We can see that real and imaginary anomaly reverses polarity around 300 m location. About 200 m wide (200–400 m location) bowl shaped high conducting zone can be seen from the current density section. This anomaly is also characterized by high gravity anomaly (Mohanty et. al

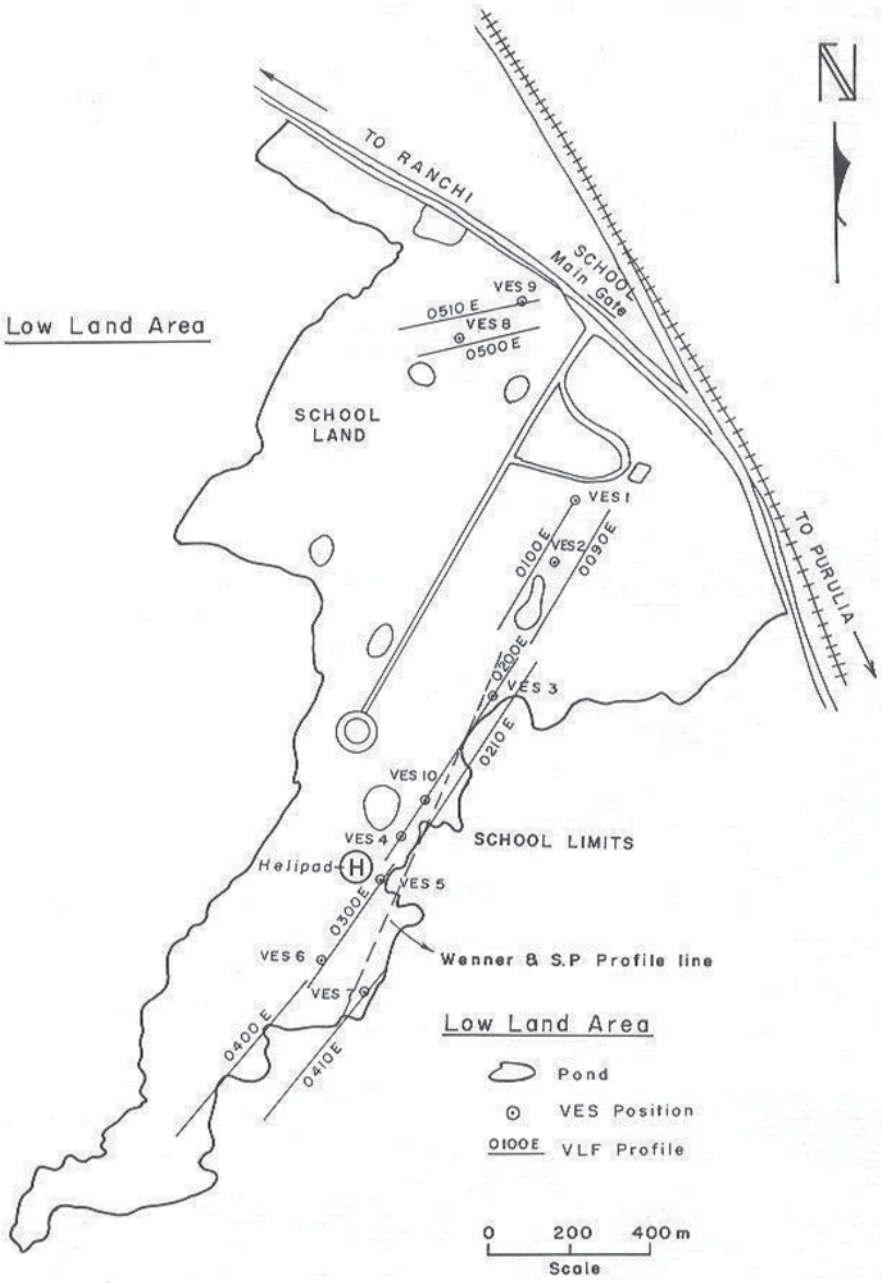

Fig. 5 Study area showing VLF profiles and other geophysical measurements. (After Sharma and Baranwal 2005)

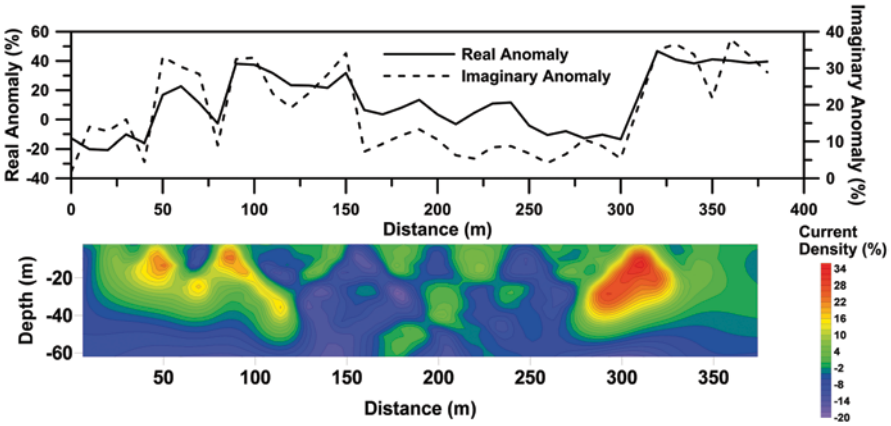

Fig. 6 VLF real anomaly and apparent current density cross-section. (Sharma and Baranwal 2005)

2011). Hence, high density and high conducting structure in the present study area reveals chromite formation. Therefore, VLF and gravity methods can be used for rapid investigation of high density metallic mineral deposit whether it is chromite or any other mineral.

Uranium Investigation

Uranium mineralization could occur in different shapes (vertical or horizontal sheet) and sizes depending on the depositional environment. The VLF EM method that suits well for delineation of vertical and gently dipping structures could also be helpful in identifying the conducting structures associated with shear zones. South Purulia Shear Zone (SPSZ), an east-west trending and almost 150 km in length, is a probable source of uranium mineralization. Beldih is an important location for apatite mining, and is exactly located along South Purulia Shear Zone (SPSZ). Particularly, the mine area consists of quartz-magnetite-apatite rocks, kaolin rocks, granite, quartzite, carbonatite, syenites, ultramafics, and some other rocks of early mesoproterozoic age. VLF survey is performed to find the location of the conductor associated with uranium mineralization, and subsequently, the extension of the body in lateral direction.

Figure 9 shows the real and imaginary VLF anomaly and current density section along a known uranium mineralization near Beldih mine. It reveals two prominent conducting features, first near −110 m location and other near +50 m location. The first conductor is shallow and anomaly is very sharp. This conductor is shallow due to power line disturbance. Second conductor coincides well with the uranium mineralization. Several VLF profiles were carried out on either side of this profile and continuation of the possible mineralization zone is depicted. It is important to highlight that only VLF survey is not enough to confirm the uranium mineralization.

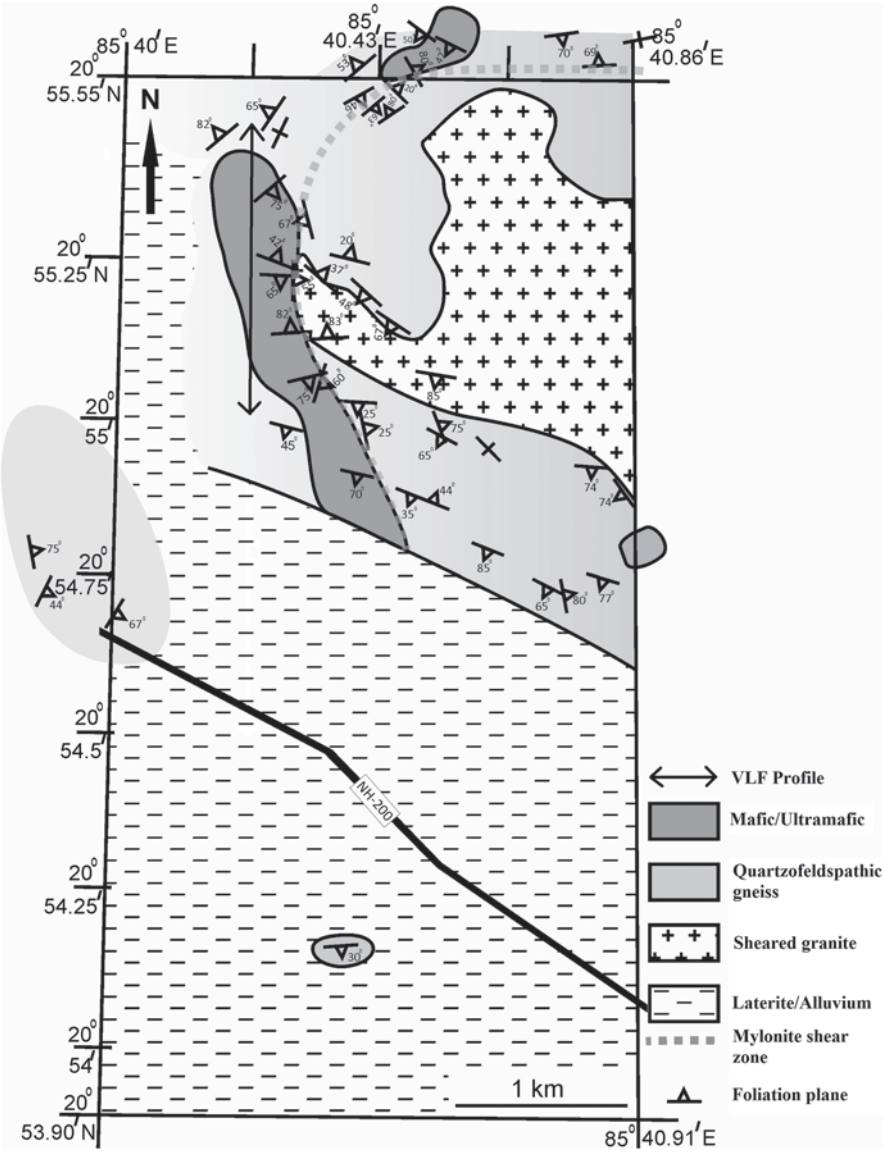

Fig. 7 Geological map of the study area. (After Mohanty et al. 2011)

Geophysical surveys such as gravity, magnetic, electrical, are necessary to confirm the extension of mineralization. This is because conductor in the area may be due to groundwater filled fractures or due to mineralization. VLF method will not be able to discriminate between these two types of conductor.

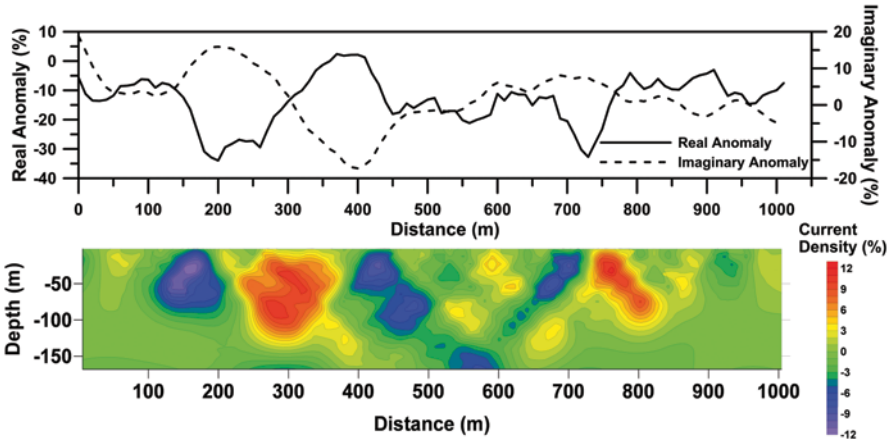

Fig. 8 Real and imaginary anomaly and current density along a profile over chromite deposit

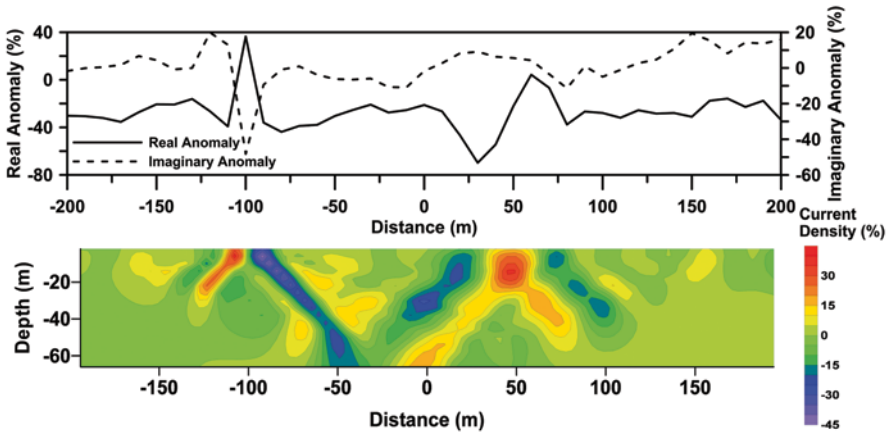

Fig. 9 Real and imaginary anomaly and current density along a profile over uranium deposit

Graphite Investigation

Graphite is an important non-metallic mineral which possesses an excellent electrical conductivity. Graphite also occurs in thin vertical as well as dipping sheet type structures. CGGC also hosts a number of graphite deposits. VLF survey was carried out over an existing graphite mine near Daltanganj (Jharkhand) India.

The study area exhibits a number of graphite mines. Mining in the area is being done mostly with open cast approach. Graphite veins are exposed in the area and mining companies are taking clue for it and digging randomly. This often results in failure and also getting poor quality graphite. It is necessary to do surveys and plan mining accordingly.

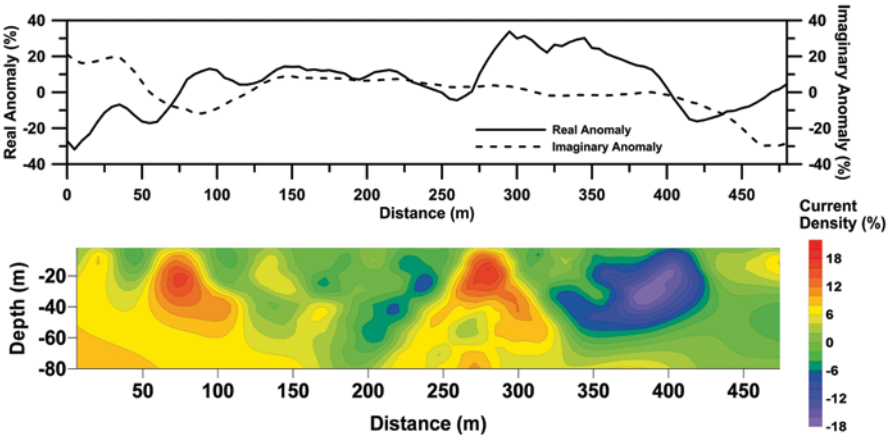

Fig. 10 Real and imaginary anomaly and current density along a profile over graphite deposit

Unplanned mining has resulted in bad quality graphite as well as loss of money due to very limited amount of graphite at several places. Figure 10 shows a VLF profile that passes nearly three exposed veins at 20, 80, and 150 m locations. Clearly, only the anomaly at the 80 m location is worth mining using open cast approach. We can see one prominent VLF anomaly near the 280 m location and one small anomaly near the 330 m location. These two bodies are not exposed on the surface but are located very close to the surface. Body at the 280 m location is the best on this profile and can be mined using open cast approach. A number of VLF profiles can help in the proper identification and to use the graphite deposit judiciously with minimum destruction to the nature.

Once again it is important to highlight that graphite deposits also exhibit strong self-potential anomaly. Therefore, self-potential survey is required to confirm the VLF anomaly due to graphite or simply due to water at the contact of hard rocks present in the area. Presence of good quality graphite, 38 %, is established for the 280 m target.

5.3 Landslide Studies

The VLF method can also be applied for landslide studies and monitoring. A VLF survey is carried out at Lantakhola landslide, Sikkim, India. Lantakhola is located approximately 74 km from the state capital Gangtok on the North Sikkim Highway, and is one of the most dangerous landslides on this highway. A number of profiles are selected on the hill slope, and the VLF measurements were carried out. It is important to mention that water flowing channels disappear on the way from hill scarf to the road level. It was important to depict the location of these channels in the subsurface for any mitigation work. Figure 11 clearly depicts the location of the

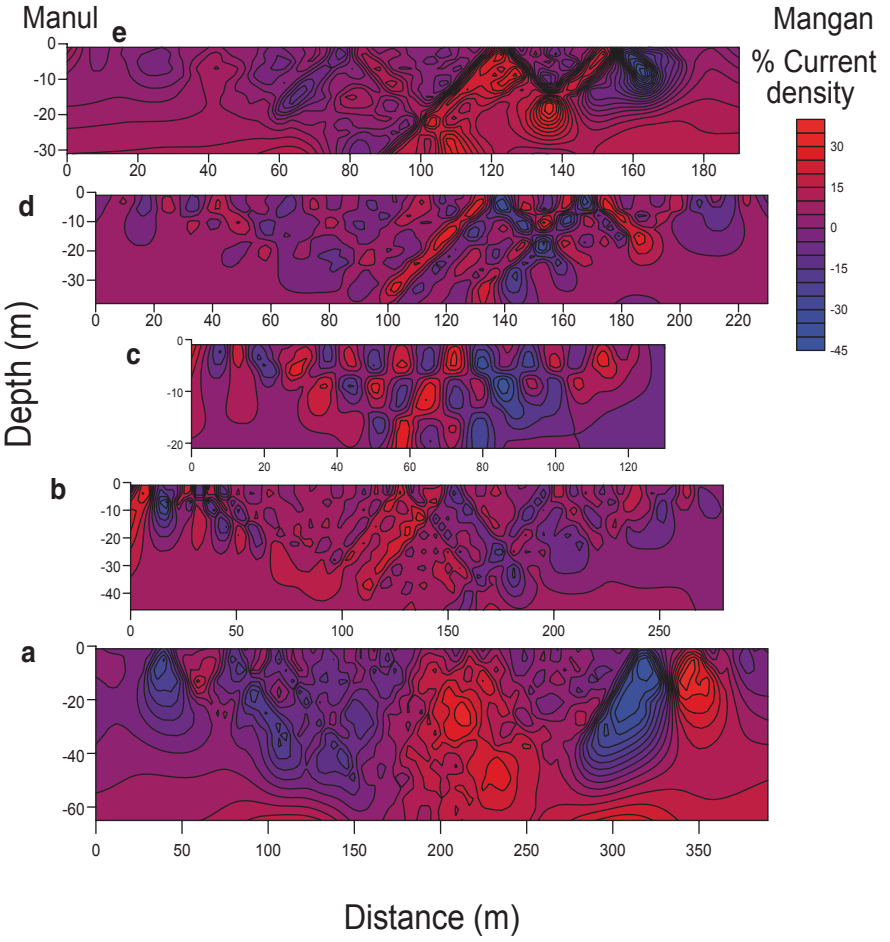

Fig. 11 VLF current density section along five profiles on Lantakhola landslide. (Sharma et al. 2010)

water channel passing below each profile. Figure 11a, which shows the results of VLF profile at the road level, also depicts the two stable regions on either side of the main landslide which can be used to build some stable structures such as a bridge for uninterrupted traffic movement on this strategic highway.

5.4 Subsurface Pollution Studies

Natural or man-made hazardous substances leaching through the subsurface fractures contaminate the underground fresh aquifer systems. Detection and regular monitoring of the area around such hazardous zones using VLF EM method is pos-

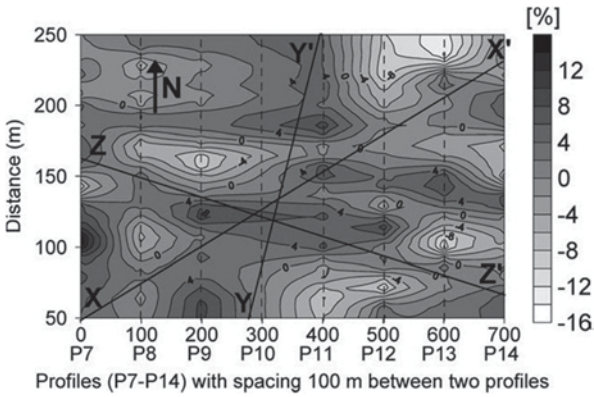

Fig. 12 Plan view of current density at 20 m depth near Tarbalu hot spring. (After Baranwal and Sharma 2006)

sible to prevent the adverse effect of subsurface pollution. Two case studies have been presented to demonstrate the efficacy of VLF EM method in such studies.

The first example consists of fluoride contamination resulting from Tarbalu hot spring, Orissa, India. Hot water gets continuously discharged though several natural openings in this area. The hot water is enriched with fluorite and also moved through subsurface fractures towards the surrounding villages. A detailed VLF study was performed around this hot spring. Plan view of current density at 20 m depth along various profiles (P7-P14) was contoured. The hot spring is located 50 m away from the bottom left corner of the Fig. 12.

It is interesting to note that high current density indicates that the fractures are filled with fluoride-contaminated groundwater. The villages marked in the direction of solid lines are affected by a high concentration of fluoride. Nearly 12 ppm fluoride has been detected in this area. Once the direction is delineated, appropriate measures can be taken to stop the contamination or to drill tube wells in another safe region.

The second example related to subsurface pollution deals with uranium mine tailings pond near Jaduguda, Jharkhand, India. Jaduguda uranium mine processes uranium ore from various uranium mines located in this region, and dumps the tailing in the nearby hills by designing suitable storage ponds. VLF survey was performed over a tailing pond to know the subsurface characteristics and any leaching of contaminated groundwater in the neighboring villages.

VLF measurements were performed along five profiles over a uranium tailing pond which is completely filled and capped with soil cover, since rainwater comes in this area from adjoining hills and runs through the tailing. Rainwater movement as well as seepage from nearby hills through tailings may contaminate groundwater in this region. Several fractures have been delineated in this area (Fig. 13). A plan view at 10 and 20 m depth was also prepared over the pond as shown in Fig. 14. It reveals that rainwater moves from the upper surface only. Current densities at 20 m depth suggest that the pond is safe and contamination is not taking place at depth. A suitable check dam can be made to avoid the flow at shallower level only.

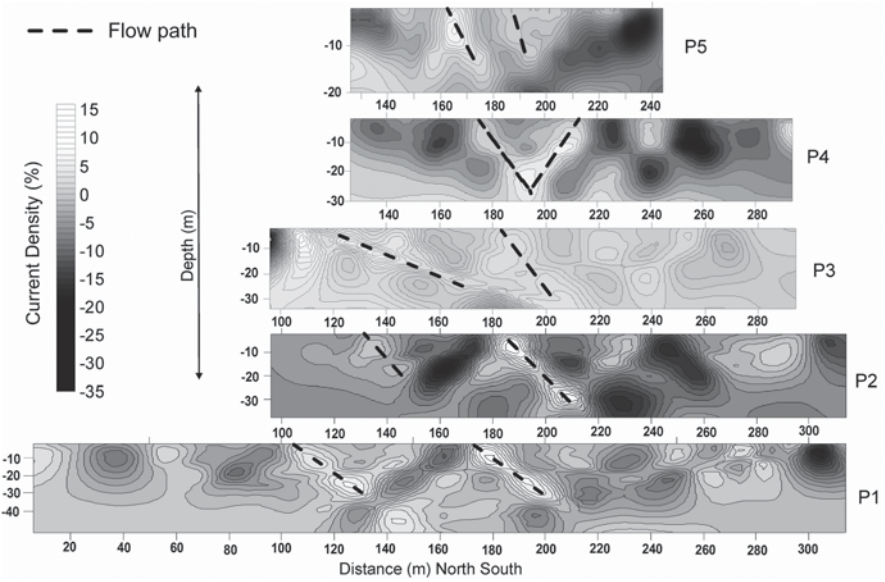

Fig. 13 Current density along various VLF profile over a tailing pond

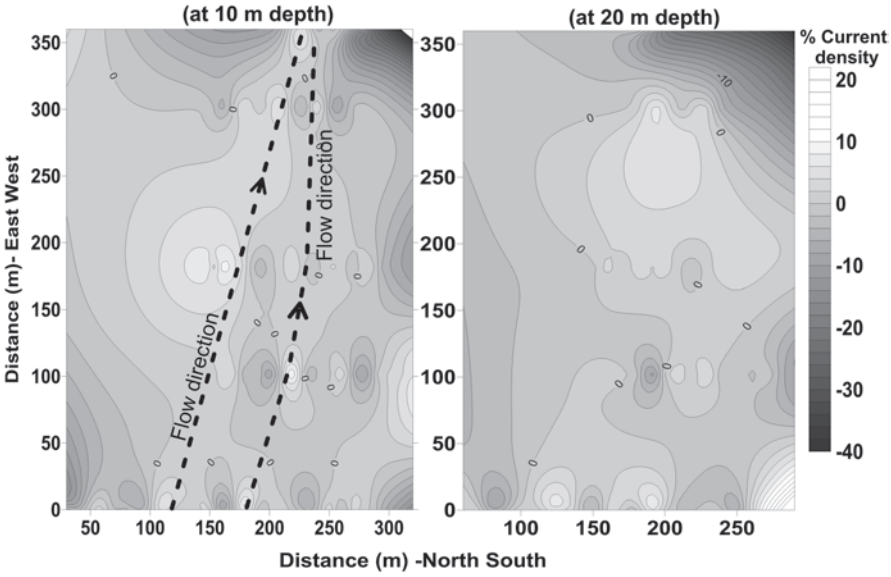

Fig. 14 Plan view of current density at 10 and 20 m depth, respectively

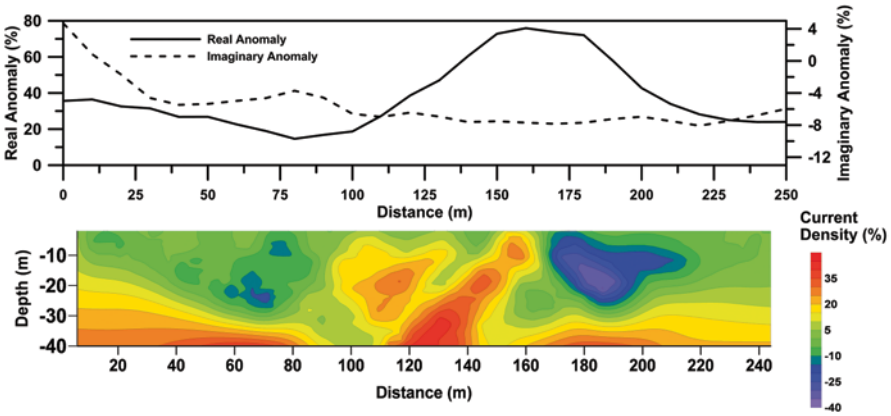

Fig. 15 VLF anomaly and current density near Bhangur chromite mine

5.5 Underground Mining Seepage

Massive seepage of groundwater in underground mines is one of the serious problems faced by mining industries. Several accidents are reported worldwide regarding flooding in the underground mines. Dewatering and discharging water to nearby big ponds are also dangerous, if these ponds are connected with fractures leading toward the underground mine. A VLF study is presented over a mine dealing with chromite mining activity near Bhangur, Orissa, India. Major fracture zones are often related with chromite formation. These fractures can be easily mapped using VLF EM method and mining planning should be done accordingly.

A VLF survey was performed near Bhangur mine in the anticipation that groundwater entering the mine is coming from a nearby big storage pond managed by another mining company. The survey was performed along a profile passing between Bhangur mine and water storage pond. Figure 15 shows the measured anomaly and inferred current density section. There is a massive fracture that connects the pond and Bhangur mine. The dip of the fracture is roughly 45° and it matches well with the dip seen in the underground mine. The study concludes that this pond will continue to create problems for Bhangur Mine.

The study demonstrates that such studies are required before the execution of any mining activity.

6 Conclusions

VLF EM method is a rapid investigation tool for shallow subsurface investigation. It has versatile applications in various explorations as well as environmental applications related with subsurface studies. Its applications have been demonstrated for

groundwater exploration, mineral investigation, landslide studies, subsurface contamination studies and monitoring, and underground mine seepage studies. Even though VLF is a rapid technique for subsurface investigation, use of complementary geophysical methods such as gravity, DC resistivity, self potential, radiometric, etc., reduces the ambiguity in the interpretation and yields reliable subsurface information.

References

Baranwal VC, Sharma SP (2006) Integrated geophysical studies in the East-Indian geothermal province. Pure Appl Geophys 163:209–227

Beamish D (1994) Two-dimensional, regularised inversion of VLF data. J Appl Geophys 32:357–374

Beamish D (2000) Quantitative 2D VLF data interpretation. J Appl Geophys 45:33–47

Becken M, Pedersen LB (2003) Transformation of VLF anomaly maps into apparent resistivity and phase. Geophysics 68:497–505

Chouteau M, Zhang P, Chapellier D (1996) Computation of apparent resistivity profiles from VLF-EM data using linear filtering. Geophys Prospect 44:215–232

deGroot-Hedlin C, Constable S (1990) Occam's inversion to generate smooth, two-dimensional models from magnetotelluric data. Geophysics 55:1613–1624

Fraser DC (1969) Contouring of VLF-EM data. Geophysics 34:958–967

Gharibi M, Pedersen LB (1999) Transformation of VLF data into apparent resistivities and phases. Geophysics 64:1393–1402

Kaikkonen P (1979) Numerical VLF modeling. Geophys Prospect 27:815–834

Kaikkonen P, Sharma SP (1998) 2-D nonlinear joint inversion of VLF and VLF-R data using simulated annealing. J Appl Geophys 39:155–176

Kaikkonen P, Sharma SP (2001) A comparison of performances of linearized and global nonlinear 2-D inversions of VLF and VLF-R electromagnetic data. Geophysics 66:462–475

Karous M, Hjelt SE (1977) Determination of apparent current density from VLF measurements. Department of Geophysics, University of Oulu, Contribution No 89, pp 1–81

Karous M, Hjelt SE (1983) Linear filtering of VLF dip-angle measurements. Geophys Prospect 31:782–794

McNeill JD, Labson VF (1991) Geological mapping using VLF radio fields. In: Nabighian MN (ed) Electromagnetic methods in applied geophysics II. Society of Exploration Geophys, pp 521–640.

Mohanty WK, Mandal A, Sharma SP, Gupta S, Misra S (2011) Integrated geological and geophysical studies for delineation of chromite deposits: a case study from Tangarparha, Orissa, India. Geophysics 76:B173–B185

Monteiro Santos FA, Mateus A, Figueiras J, Gonçalves MA (2006) Mapping groundwater contamination around a landfill facility using the VLF-EM method—a case study. J Appl Geophys 60:115–125

Ogilvy RD, Lee AC (1991) Interpretation of VLF-EM in-phase data using current density pseudosections. Geophys Prospect 39:567–580

Oskooi B, Pedersen LB (2005) Comparison between VLF and RMT methods: a combined tool for mapping conductivity changes in the sedimentary cover. J Appl Geophys 57:227–241

Oskooi B, Pedersen LB (2006) Resolution of airborne VLF data. J Appl Geophys 58:158–175

Parasnis DS (1986) Principles of applied geophysics. Chapman and Hall, London

Paterson NR, Ronka V (1971) Five years of surveying with the very low frequency electromagnetic method. Geoexploration 9:7–26

Pedersen LB, Becken M (2005) Equivalent images derived from very-low-frequency (VLF) profile data. Geophysics 70:G43–G50

Pedersen LB, Oskooi B (2004) Airborne VLF measurements and variations of ground conductivity: a tutorial. Surv Geophys 25:151–181
Press WH, Teukolsky SA, Vetterling WT, Flannery BP (1992) Numerical recipes in C: the art of scientific computing. Cambridge University, New York
Rodi WL, Mackie RL (2001) Nonlinear conjugate gradient algorithm for 2-D magnetotelluric inversion. Geophysics 66:174–187
Sasaki Y (1989) Two-dimensional joint inversion of magnetotelluric and dipole-dipole resistivity data. Geophysics 54:254–262
Sharma SP, Baranwal VC (2005) Delineation of groundwater bearing fracture zones in a hard rock area integrating very low frequency electromagnetic and resistivity data. J Appl Geophys 57:155–166
Sharma SP, Anbarasu K, Gupta S, Sengupta A (2010) Integrated very low frequency EM, electrical resistivity and geological studies on the Lanta Khola landslide, North Sikkim, India. Landslides 7(1):43–53
Sharma SP, Kaikkonen P (1998a) Two-dimensional nonlinear inversion of VLF-R data using simulated annealing. Geophys J Int 133:649–668
Sharma SP, Kaikkonen P (1998b) An automatic finite element mesh generation and element coding in 2-D electromagnetic inversion. Geophysica 34:93–114
Siripunvaraporn W, Egbert G (2000) An efficient data-subspace inversion method for 2-D magnetotelluric data. Geophysics 65:791–803
Smith BD, Ward SH (1974) On the computation of polarization ellipse parameters. Geophysics 39:867–869
Wannamaker PE, Stodt JA, Rijo L (1987) A stable finite element solution for two-dimensional magnetotelluric modeling. Geophys J R Astron Soc 88:277–296